

303925

TEMPERATURE DEPENDENCE OF ULTRAVIOLET ABSORPTION
CROSS-SECTIONS OF ALTERNATIVE HYDROCHLOROFLUOROCARBONS.

D. GILLOTAY, P. C. SIMON and L. DIERICKX

INSTITUT D'AERONOMIE SPATIALE DE BELGIQUE.
3, Avenue Circulaire, B-1180 BRUSSELS, BELGIUM.

ABSTRACT

Ultraviolet absorption cross-section of six alternative hydrochlorofluorocarbons (HCFC-21, HCFC-22, HCFC-123, HCFC-124, HCFC-141b and HCFC-142b) and of one alternative hydrobromofluorocarbon (Halon-22b1) have been measured between 170 and 260 nm for temperature ranging from 210 to 295 K. These data are compared with other available determinations performed at room temperature. and their temperature dependence is discussed. Photodissociation coefficients are estimated and their temperature dependence is discussed. Impact of the photodissociation on the total atmospheric destruction of these compounds is illustrated.

I. INTRODUCTION.

Since the 'Montreal Protocole on substances that deplete the ozone layer', alternative CFCs are actively pursued to replace classical CFCs and Halons in many of their applications. Among them, partially hydrogenated halocarbons are relatively vulnerable to OH radical attack at tropospheric altitude which will remove a great part of them before reaching the stratosphere where the remaining HCFC molecules will be photolysed or will react with OH or O(¹D) radicals.

Determination of lifetime and ozone depletion potential of these molecules require an accurate knowledge of the UV absorption cross-sections as a function of wavelength and temperature. The purpose of this paper is to compare available absorption cross-section data of HCFCs, to discuss their temperature dependence and to show the importance of the photolysis in the remove of these alternative compounds in the troposphere and the stratosphere. New investigations of cross-sections of Halon-22b1 will also be presented.

II. EXPERIMENTAL.

Ultraviolet absorption cross-sections and their temperature-dependence were determined by means of a double beam experimental device previously described (Gillotay et al., 1988) which includes a 40W-deuterium lamp or a FEL 1000W tungsten filament lamp as light

source, a 1 m Mc Pherson 225 monochromator, 200 cm and 20 cm thermostated absorption cells (one of them being used as reference channel), EMR type 542 P-09-18 solar blind photomultipliers, and a data acquisition system. The bandwidth is 0.1 nm and the wavelength repeatability ± 0.01 nm. The pressure inside the cell ranging from 2×10^{-3} to 1×10^3 Torr, is measured by means of three capacitance MKS Baratron manometers 170-315 with a 1, 10, and 1000 Torr full scale range. A regular calibration of these manometers allows a precision better than ± 0.1 %. Low temperatures are determined with absolute uncertainties of around ± 1 K and a temperature stability of around ± 0.3 K is usually observed. The purity of the seven compounds is better than 99.5 % as determined by gas phase chromatography.

III. RESULTS.

Numerical values of absorption cross-sections for wavenumber intervals of 500 cm^{-1} have already been reported for the six HCFCs (Simon et al., 1988, Gillotay and Simon, 1991a, 1991b) and are given in table I for Halon-22b1.

In all cases, Beer-Lambert's law was verified for absorption ranging from 10 to 85 %. In such conditions, and according to the error budget previously published, (Simon et al., 1988), the absorption cross-sections reported here are determined with an accuracy of ± 2 % at room temperature and of ± 3 to ± 4 % at the lowest temperature.

Halon-22b1 display a continuous absorption spectra with a maximum around 200nm and a temperature dependence already observed in the case of other Halon, increase of the absorption cross-sections with the temperature for the smaller wavelengths and near the maximum and decrease of these cross-sections for the longer wavelengths.

The relative absorption cross-sections at room temperature of HCFC-123, HCFC-124, HCFC-141b and HCFC-142b are illustrated in Figures 1-4 (Ref = WHO,1990) and show large discrepancies up to 60 % for HCFC-123, for the low values of absorption. In addition, some reported temperature dependence are not coherent with the usual exponential decrease of cross-section values at low temperature. These two issue raise question on the experimental uncertainties when measuring low optical thickness values

IV. DISCUSSION.

Photodissociation coefficients of the molecules have been calculated, neglecting the effects of multiple scattering, for given altitude (z), zenith angle (χ) and wavelengths intervals according to the relation :

$$J(z) = \sigma_{\lambda} q_{\lambda}(z) \quad ; \quad q_{\lambda}(z) = q_{\lambda}(\infty) e^{-\tau_{\lambda}(z)}$$

$$\tau_{\lambda}(z) = \int_z^{\infty} [n(O_2) \sigma_{\lambda}(O_2) + n(O_3) \sigma_{\lambda}(O_3) + n(\text{air}) \sigma_{\text{scatt}}] \sec \chi dz$$

where

z is the altitude,

σ are the absorption cross-sections,

$q_{\lambda}(z)$ and $q_{\lambda}(\infty)$ are the solar irradiance at altitude z or extraterrestrial ($z = \infty$)

n is the number of particles per volume unit.

Calculations are made for solar zenith angle of 0° and 60° ($\sec = 1$ and 2), taking into account the values of $\sigma(O_2)$ and $\sigma(O_3)$ from WMO and Kockarts (1976), σ_{scatt} from Nicolet (1984) and the values of $q(\infty)$ from WMO (1986) and by taking into account the actual values of cross-sections corresponding to the temperature conditions at each altitude.

The loss rates calculated with the WMO rate constants and the photodissociation coefficients corresponding to the temperature conditions at each altitude are represented as a function of altitude in Figures 5-11. These figures show clearly the importance of photolysis relative to the reaction with OH and $O(^1D)$ radicals. At tropospheric altitude, reaction with OH and $O(^1D)$ are in all the cases the main removal mechanisms. Photolysis becomes the main process in the stratosphere for HCFC-123, HCFC-141b and Halon-22b1, but remains of lower or equal importance for all the other compounds.

V. REFERENCE.

- ALLIED-SIGNAL CORPORATION, 1989, in WMO report 20
- GILLOTAY D., A. JENOUVIER, B. COQUART, M.F. MERIENNE, and P.C. SIMON, 1898, Ultraviolet absorption cross-sections of Bromoform in the temperature range 295-240 K., Planet. Space Sci., 37, 1127-1140.
- GILLOTAY D. and P.C. SIMON, 1991a Temperature dependence of ultraviolet absorption cross-sections of alternative chlorofluoroethanes., J. Atmos. Chem., 12, 269-285.
- GILLOTAY D. and P.C. SIMON, 1991b Temperature dependence of ultraviolet absorption cross-sections of alternative chlorofluoroethanes. 2. The 2-chloro-1,1,1,2 tetrafluoro ethane - HCFC-124., J. Atmos. Chem., 13, 289-299.
- HUBRICH, C. and F. STUHL, 1980, The ultraviolet absorption of some halogenated methanes and ethanes of atmospheric interest., J. Photochem., 12, 93-107.
- KOCKARTS G., 1976, Absorption and photodissociation in the Schumann-Runge bands of molecular oxygen in terrestrial atmosphere., Planet. Space Sci., 24, 589-604
- ORLANDO, J.J., J.B. BURKHOLDER, S.S. McKEEN and A.R. RAVISHANKARA, 1990, the atmospheric fade of several hydrochlorofluoroethanes 2. Temperature dependence of UV absorption cross sections and atmospheric lifetimes., J. Geophys. Res., 96, 5013-5023.
- MOLINA M.J. and L.T. MOLINA, 1989, in WMO report 20.
- NICOLET M., 1984, On the molecular scattering in the terrestrial atmosphere : an empirical formula for calculation in the homosphere., Planet. Space Sci., 32, 1467-1468.
- SIMON P.C., D. GILLOTAY, N. VANLAETHEM-MEUREE, and J. WISEMBERG, 1988, Ultraviolet absorption cross-sections of chloro and chlorofluoromethanes at stratospheric temperatures., J. Atmos. Chem., 7, 107-1345.
- WMO, 1986, Atmospheric ozone 1985, WMO global ozone research and monitoring project, Report 14.
- WMO, 1990, Scientific assessment of stratospheric ozone, 1989, Report 20, Volume II.

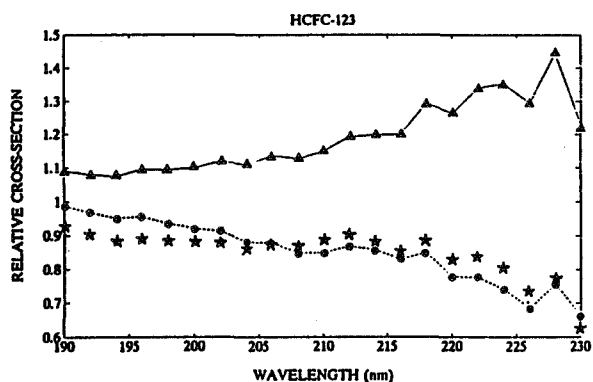


Figure 1

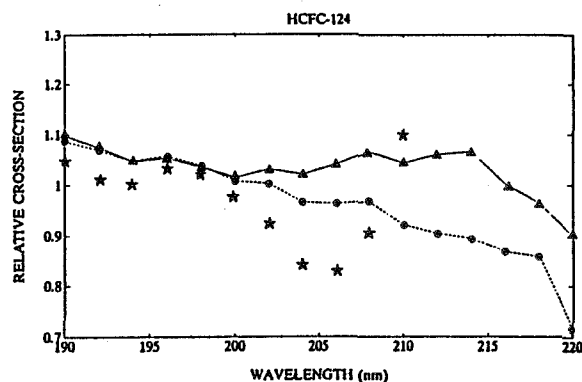


Figure 2

Figures 1-4 Relative absorption cross-sections

- ▲ : Gillotay and Simon, 1991a, 1991b.
 ● : Molina and Molina, 1989.
 * : Allied-Signal Corporation, 1989.
 + : Hubrigh and Stuhl, 1980.

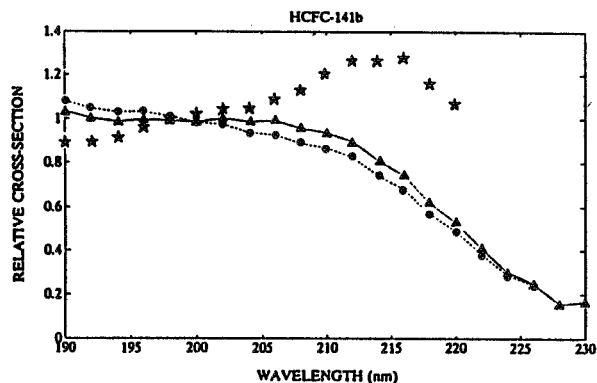


Figure 3

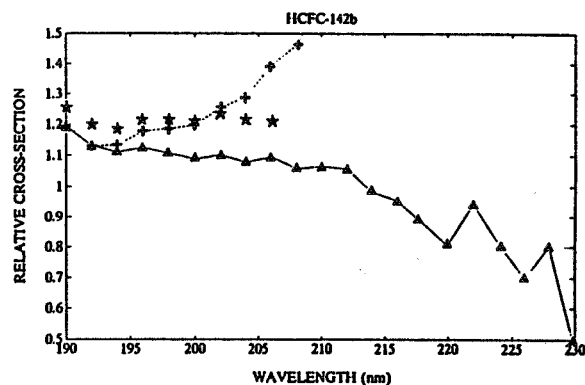


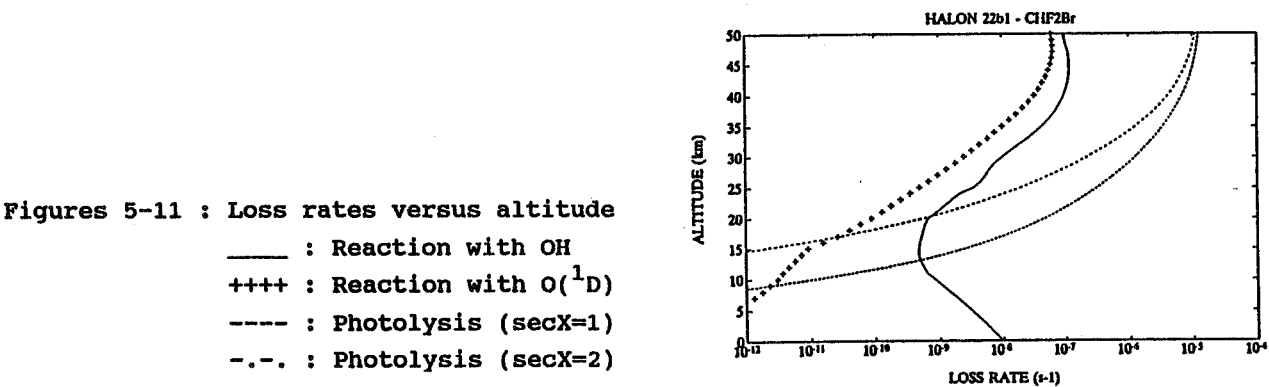
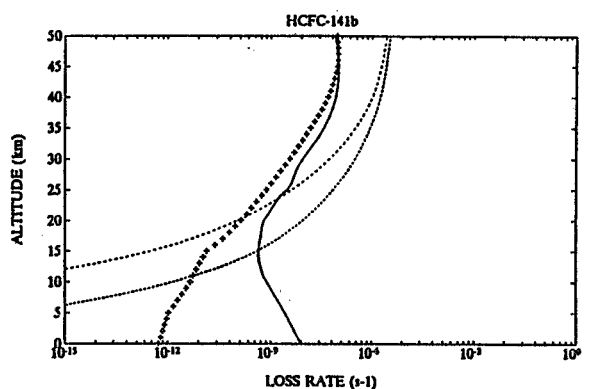
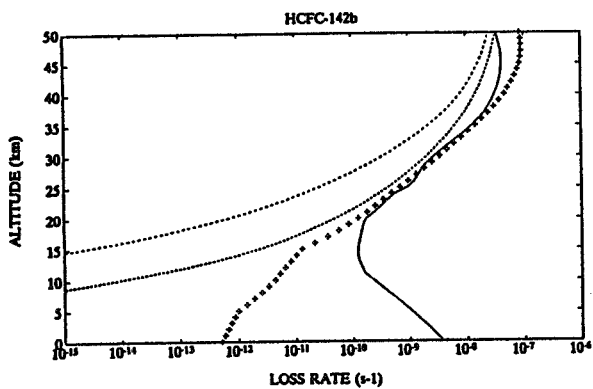
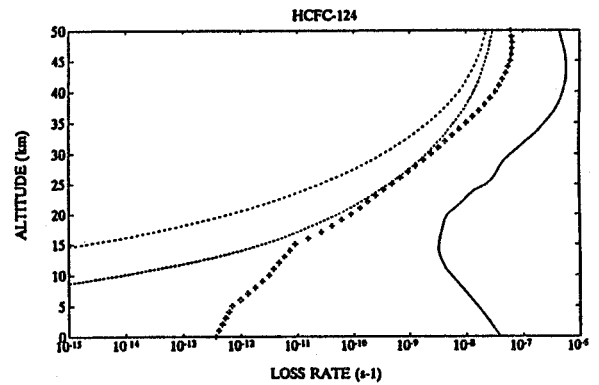
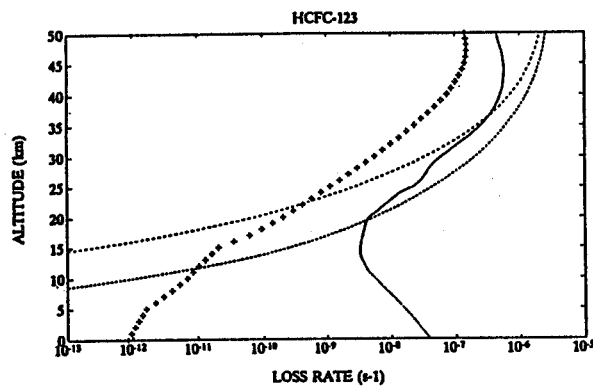
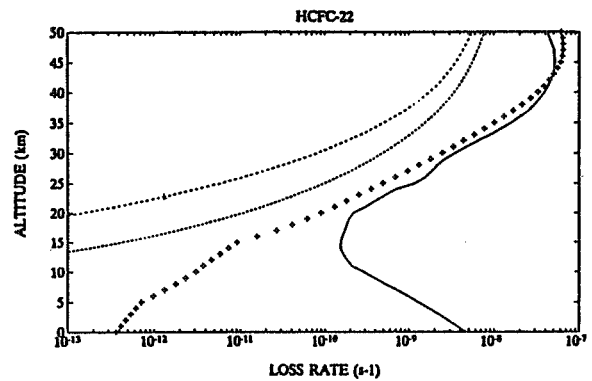
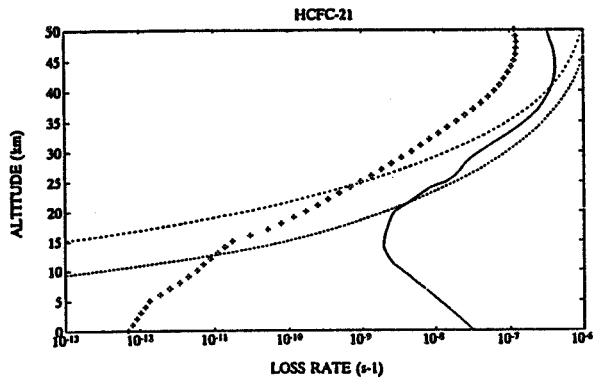
Figure 4

Figures 1-4 Relative absorption cross-sections

- ▲ : Gillotay and Simon, 1991a, 1991b.
- : Molina and Molina, 1989.
- * : Allied-Signal Corporation, 1989.
- + : Hubrish and Stuhl, 1980.

Table I CHF₂Br - Halon 22b1

		$\sigma(\lambda) \times 10^{21} \text{ (cm}^2 \text{ molec.}^{-1}\text{)}$				
N°	(nm)	295K	270K	250K	230K	210K
42	166.7-169.5	39.7	47.2	54.2	62.2	71.5
43	169.5-172.4	82.1	89.9	96.7	104	112
44	172.4-173.9	125	131	137	143	149
45	173.2-175.4	156	162	166	171	175
46	175.4-177.0	188	191	196	200	204
47	177.0-178.6	219	223	226	229	232
48	178.6-180.2	245	249	253	257	260
49	180.2-181.8	266	272	277	282	287
50	181.8-183.5	283	291	298	305	312
51	183.5-185.2	296	304	311	318	325
52	185.2-186.9	306	314	320	327	333
53	186.9-188.7	314	322	328	334	340
54	188.7-190.5	320	327	333	339	346
55	190.5-192.3	323	330	336	343	349
56	192.3-194.2	323	330	336	343	349
57	194.2-196.1	319	327	333	339	346
58	196.1-198.0	312	320	326	332	338
59	198.0-200.0	301	309	315	321	327
60	200.0-202.0	286	294	299	305	311
61	202.0-204.1	268	275	280	286	291
62	204.1-206.2	247	253	258	262	267
63	206.2-208.3	224	229	233	236	240
64	208.3-210.5	200	203	206	209	211
65	210.5-212.8	174	176	177	179	181
66	212.8-215.0	149	149	150	150	151
67	215.0-217.4	124	124	123	123	122
68	217.4-219.8	101	99.6	98.3	97.1	95.9
69	219.8-222.2	80.6	78.3	76.5	74.8	73.1
70	222.2-224.7	62.6	59.9	57.9	55.9	53.9
71	224.2-227.3	47.1	44.3	42.1	40.1	38.2
72	227.3-229.9	34.5	31.7	29.7	27.8	26.1
73	229.9-232.6	24.5	22.1	20.3	18.7	17.2
74	232.6-235.3	16.9	14.9	13.4	12.1	10.9
75	235.3-238.1	11.4	9.73	8.59	7.58	6.69
76	238.1-241.0	7.41	6.17	5.33	4.60	3.97
77	241.0-243.9	4.62	3.73	3.15	2.66	2.24
78	243.9-246.9	2.82	2.22	1.83	1.50	1.24
79	246.9-250.0	1.65	1.26	1.01	0.814	0.655
80	250.0-253.2	0.963	0.715	0.564	0.445	0.351
81	253.2-256.4	0.525	0.381	0.294	0.228	0.176
82	256.4-259.7	0.288	0.205	0.156	0.119	0.0909
83	259.7-263.2	0.148	0.104	0.0788	0.0596	0.0450
84	263.2-266.7	0.0755	0.0533	0.0403	0.0305	0.0231



Figures 5-11 : Loss rates versus altitude
 — : Reaction with OH
 +++ : Reaction with O(¹D)
 ---- : Photolysis (secX=1)
 -.-. : Photolysis (secX=2)